Modeling and Optimization of Fixed-Bed Fischer-Tropsch Synthesis Using Genetic Algorithm

Arezoo Sadat Emrani[*1], Mohammad Saber[2], Fatola Farhadi[1]

[1] Department of Chemical and Petroleum Engineering, Sharif University of Technology, Tehran, Iran

[2] Department of Energy Engineering, Sharif University of Technology, Tehran, Iran

Abstract

In this paper, modeling and optimization of Fischer-Tropsch Synthesis is considered in a fixed-bed catalytic reactor using an industrial Fe-Cu-K catalyst. A one dimensional pseudo-homogenous plug flow model without axial dispersion is developed for converting syngas to heavy hydrocarbons. The effects of temperature, pressure, H_2 to CO ratio in feed stream, and CO molar flow on the mass flow rate of the desired product (C_{5+}) are investigated. Since the Fischer-Tropsch synthesis produces a wide range of hydrocarbon products, it is important to optimize the reactor operating parameters and feed conditions to maximize yield of reactor. Genetic algorithm was used as the optimization algorithm in this study. The processing variables are defined in the following ranges: Temperature: 493-542 K, Pressure: 10.9-30.9 bar, CO molar flow: 0.0815-0.3074 gmole/s and the H_2/CO feed ratio: 0.98-2.99. A reactor model was developed and along with appropriate reaction kinetics, the performance of the reactor was investigated. Model results were in good agreement with experimental data. After validating the model, the production of C_{5+} was optimized. The results indicated that the production of C_{5+} increased with increasing pressure while it decreased with increasing temperature, H_2/CO ratio, and CO molar flow rate in the feed stream.

Keywords: Fischer-Tropsch synthesis, Fixed-bed reactor, Genetic algorithm, Modeling, Optimization

Introduction

Fischer-Tropsch synthesis (FTS) converts syngas into a wide range of products including linear hydrocarbons and oxygenates. It is a promising and environmentally friendly option for production of transportation fuels such as gasoline and diesel from biomass, coal and natural gas. Various types of reactors (including fixed-bed, fluidized-bed and slurry phase) have been considered in the history of FTS process development [1]. The fixed-bed type reactor is one of the innovations being used in an industrial scale by Sasol over an iron-based catalyst [2] and by Shell [3].

Modeling of fixed-bed Fischer-Tropsch reactor has been performed in several previous investigations. Wang et al. [1] have proposed a one-dimensional heterogeneous reactor model to investigate the performance of fixed-bed Fischer-Tropsch reactor for hydrocarbon production. Jess and Kern [4] developed a two dimensional pseudo-homogeneous model for multi-tubular reactors for FTS. The modeling of FTS using biosyngas in a single tube fixed-bed reactor over cobalt catalyst has been carried out by Rafiq et al [5].

The productivity of hydrocarbons and fluid temperature profile along the axis of the reactor has been reported in their work. Fernandes and Teles [6] have modeled a Fischer-Tropsch fixed-bed reactor with assumptions of isothermal conditions, negligible mass and heat transfer resistance between the catalyst and fluid, and the plug flow regime. They then optimized the operating conditions of the reactor to enhance the production of gasoline and diesel cuts. Since the FTS produces a wide range of hydrocarbon products, the optimization of the FTS process has been considered by some investigators [6, 7] as to maximize the production of desired product.

In addition of fixed-bed Fischer-Tropsch reactor, modeling of FTS in slurry bubble column reactors has been taken into account

---

in several studies [8]. Schweitzer and Viguié have investigated reactor modeling of a slurry bubble column for FTS with considering the gas recycle after condensation step [9]. Modeling and product grade optimization of FTS in a slurry reactor has been carried out by Fernandes [10]. Modeling and optimization of a large-scale slurry bubble column reactor for producing 10,000 bbl/day of Fischer–Tropsch liquid hydrocarbons have been investigated by Sehabiague et al [11].

In the present study, FTS and Water Gas Shift (WGS) reactions were considered in a fixed-bed reactor with a novel industrial catalyst. A one dimensional pseudo-homogenous reactor model was developed under non-isothermal and steady state conditions followed by optimization of operating conditions to maximize C_{5+} production as the desired product. The desired product (C_{5+}) has been considered to be in the range of C_{11} to C_{27}. Genetic Algorithm (GA) was used in the optimization procedure.

2. The development of the rector model

2.1. Model assumptions:

The reactor was considered as a tubular fixed-bed reactor with length L and inner diameter d_{in} packed with a bed of Fe-Cu-K catalyst. The main reactions are the following combination of FTS and WGS reactions:

1- Olefin formation reactions:
$$nCO + 2nH_2 \longrightarrow C_nH_{2n} + nH_2O \qquad (1)$$

2- Paraffin formation reactions:
$$nCO + (2n+1)H_2 \longrightarrow C_nH_{2n+2} + nH_2O \qquad (2)$$

3- Water gas shift reaction:
$$CO + H_2O \longrightarrow CO_2 + H_2 \qquad (3)$$

The main assumptions in the developed model are:

1- Non-isothermal condition is assumed as there is a considerable temperature change along the reactor.

2- Pressure drop across the bed is insignificant with the particle sizes and flow rates employed in this study (Wang et al., 2003).

3- A one dimensional plug flow model without axial dispersion.

The intrinsic reaction rates over an industrial Fe-Cu-K catalyst proposed by Wang et al. [12] were used in this study. It should be noted that, to match the conditions of the exclusion of intra-particle and external diffusion limitations, the kinetics experiments are performed by using small particle sizes and high space velocities. The sizes of catalyst particle used are within the recommended size range (<0.2 mm) for intrinsic FTS kinetics measurements [12].

2.2. Mathematical model

A one-dimensional pseudo-homogenous model was selected to simulate a tubular fixed-bed Fischer-Tropsch reactor. The reactor is therefore a multi-tubular shell with boiling water as the coolant in the shell. The mass and energy balance equations for the bulk gas phase could be written as follows [13]:

$$u_s C_{pm} \rho_g \frac{dT}{dZ} = \rho_p(1 - \varepsilon_B) \sum_{j=1}^{NR}(-\Delta H_j)R_j + 4\frac{U}{d_{in}}(T_w - T_g) \qquad (4)$$

$$\frac{d(U_s C_i)}{dz} = \rho_p(1 - \varepsilon_B)R_j \qquad (5)$$

The initial conditions for the inlet bulk phase were:
At Z=0: $C_i = C_{i,0}$, $P=P_{in}$, $T_g = T_{in}$

The mass and energy balance equations were solved with an ODE solver in MATLAB environment. The preferred fixed-bed reactor type is multi-tubular with the catalyst placed inside the tubes and cooling medium (pressurized boiling water) on the shell sides within the range of 503-533 K [14].

The tube-side heat transfer coefficient (h_i) and the shell-side heat transfer coefficient (h_o) were taken into account for the

calculation of overall heat transfer coefficient (U). Moreover, h_i and h_o were calculated by Leva's correlation [15]. The superficial gas velocity (u_s) along the reactor axis was calculated based on the total mass flux and the local density of the gas mixture (ρ_g). The other required properties such as f_o, f_i and k_w were obtained from references [16, 17].

2.3. Kinetics of FTS and WGS reactions:

The intrinsic reaction rates for FTS and WGS reactions over an industrial Fe-Cu-K catalyst, given by equations (6) to (9), were proposed by Wang et al. [12] using an experimental reactor consisting of a stainless steel tubing with inner diameter of 18 mm and an effective bed length of approximately 300mm. Experiments were carried out by using catalyst particles with a diameter between 0.15 and 0.18 mm (80–100 ASTM mesh) (Wang et al., 2003).

Catalyst pretreatment, which essentially leads to a reduction of Fe_2O_3 to Fe_3O_4 and Fe_xC, is necessary in order to obtain an active catalyst with good stability. The crystal phase changes of the fresh and used catalysts are characterized by using Powder X-ray Diffraction (XRD) test. The results of XRD test shows that the magnetite (Fe_3O_4) is the dominant iron phase observed in the used catalysts and the peak characteristics of carbide (Fe_5C_2) are clearly evident. For the unreduced fresh catalyst, the majority of peaks can be attributed to Fe_2O_3 (Wang et al., 2003).

a) For paraffin's reactions:

$$R_{CH_4} = \frac{k_{5m}P_{H2}\alpha_1}{\left(1 + \frac{1}{K_2K_3K_4}\frac{P_{H2O}}{P_{H2}^2} + \frac{1}{K_3K_4} + \frac{1}{P_{H2}} + \frac{1}{K_4}\right)\sum_{i=1}^{N}(\prod_{j=1}^{i}\alpha_j)} \tag{6}$$

For $n \geq 2$:

$$R_{C_nH_{2n+2}} = \frac{k_5P_{H2}\prod_{j=1}^{n}\alpha_j}{\left(1 + \frac{1}{K_2K_3K_4}\frac{P_{H2O}}{P_{H2}^2} + \frac{1}{K_3K_4} + \frac{1}{P_{H2}} + \frac{1}{K_4}\right)\sum_{i=1}^{N}(\prod_{j=1}^{i}\alpha_j)} \tag{7}$$

b) For olefin's reactions:

$$R_{C_nH_{2n}} = \frac{k_6(1-\beta_n)\prod_{j=1}^{n}\alpha_j}{\left(1 + \frac{1}{K_2K_3K_4}\frac{P_{H2O}}{P_{H2}^2} + \frac{1}{K_3K_4} + \frac{1}{P_{H2}} + \frac{1}{K_4}\right)\sum_{i=1}^{N}(\prod_{j=1}^{i}\alpha_j)} \tag{8}$$

c) For WGS reaction:

$$R_{CO2} = \frac{k_v\left(P_{CO}P_{H2O}\big/P_{H2}^{0.5} - P_{CO2}P_{H2}^{0.5}\big/K_P\right)}{1 + \frac{K_vP_{CO}P_{H2O}}{P_{H2}^{0.5}}} \tag{9}$$

where α_1 and α_n are calculated from equations (10) and (11):

$$\alpha_1 = \frac{k_1P_{CO}}{k_1P_{CO} + k_{5M}P_{H2}} \quad (n = 1) \tag{10}$$

$$\alpha_n = \frac{k_1P_{CO}}{k_1P_{CO} + k_5P_{H2} + k_6(1 - \beta n)} \tag{11}$$
$(n \geq 2)$

And β_n in equation (8) is defined in by:

$$\beta_n = \left(\frac{k_{-6}}{k_6}\right) *$$

$$\left(\frac{P_{C_nH_{2n}}}{\alpha_A^{n-1}\frac{k_1P_{CO}}{k_1P_{CO} + k_5P_{H2}} + \frac{k_{-6}}{k_1P_{CO} + k_5P_{H2} + k_6}}\right) \tag{12}$$

and α_A in equation (12) is defined as:

$$\alpha_A = \frac{k_1P_{CO}}{k_1P_{CO} + k_5P_{H2} + k_6} \quad (n = 1) \tag{13}$$

Temperature dependence of the reaction rate constants are given by an Arrhenius-type equation:

$$k_i(T) = k_{i,0}\exp\left(\frac{-Ei}{RT}\right) \tag{14}$$

The equilibrium constant for the WGS reaction is estimated using equation (15):

$$\ln K_P = \frac{5078.0045}{T} - 5.8972089$$
$$+ (13.958689 \times 10^{-4})T$$
$$- (27.592844 \times 10^{-8})T^2 \tag{15}$$

Partial pressure of component i is calculated using equations (16) and (17):

$$P_i = C_0(1-X)RT, \text{ for feed} \tag{16}$$

$$P_i = C_0XRT, \text{ for paraffin and olefin} \tag{17}$$

Rate parameters are summarized in Table 1 as reported by Wang et al. [12].

3. Results and discussion

The reactor model along with the reaction kinetics outlined by Wang et al. [12] were used to investigate the effect of various operating parameters on the C_{5+} yield from the experimental reactor used by Wang et al. [12]. Typical results are presented in Figure 1 for the effect of reaction pressure and feed flow rate on the C_{5+} yield indicating that when all other parameters are remained unchanged, the C_{5+} yield would increase with increasing reactor pressure and decrease with increasing feed flow rate. Other important operating variables, including reaction temperature and the H_2 to

CO ratio in the feed, can affect the overall reactor performance and thus a set of operating conditions would exist that optimizes the performance of the reactor.

Before proceeding with the optimization algorithm to identify the optimum conditions, the validity of the reactor model along with the proposed reaction kinetics was tested using the experimental data reported by Wang et al. [12]. The agreement between predicted and experimental product flow rates are presented in Figure 2 for CO, H_2, CO_2, CH_4, H_2O, and C_{5+} products. The AARE (Absolute Average Relative Error) defined by equation (18) can be used as a criteria for model's accuracy evaluation. These are reported in Table 2 for different components indicating a fair overall agreement.

$$AARE = \frac{1}{n}\sum_{i=1}^{n}\left|\left(\frac{C(cal)_i - C(exp)_i}{C(exp)_i}\right)\right| \times 100 \tag{18}$$

Table 1: Parameter values for FT-WGS reactions [12]

Parameter	Dimension	Estimate	Parameter	Dimension	Estimate
k_1	$mol.g^{-1}.bar^{-1}.s^{-1}$	2.23×10^{-5}	$k_{v,0}$	$mol.g^{-1}.bar^{-1}.s^{-1}$	15.7
$k_{5m,0}$	$mol.g^{-1}.bar^{-1}.s^{-1}$	4.65×10^{3}	E_v	$kJ.mol^{-1}$	45.08
E_{5m}	$kJ.mol^{-1}$	92.89	k_{-6}	$mol.g^{-1}.bar^{-1}.s^{-1}$	2.75×10^{-5}
$k_{5,0}$	$mol.g^{-1}.bar^{-1}.s^{-1}$	2.74×10^{2}	K_v	$bar^{-0.5}$	1.13×10^{-3}
E_5	$kJ.mol^{-1}$	87.01	K_2	-	1.81×10^{-2}
$k_{6,0}$	$mol.g^{-1}.bar^{-1}.s^{-1}$	2.66×10^{6}	K_3	-	4.68×10^{-2}
E_6	$kJ.mol^{-1}$	111.04	K_4	-	0.226

Table 2: AARE for different components
for evaluation of predicted yields
versus experimental data by [12]

Component	AARE, %
CO	9.95
H_2	8.44
H_2O	2.31
CO_2	6.21
CH_4	5.23
C_{5+}	10.79

(a): Effect of pressure on C_{5+} yield (g/s) at
T = 518.15 K, F = 400 ml/min, H_2/CO = 1.92

(b): Effect of flow rate on C_{5+} yield (g/s) at
T = 518.15 K, P = 20.92 bar, H_2/CO = 1.94
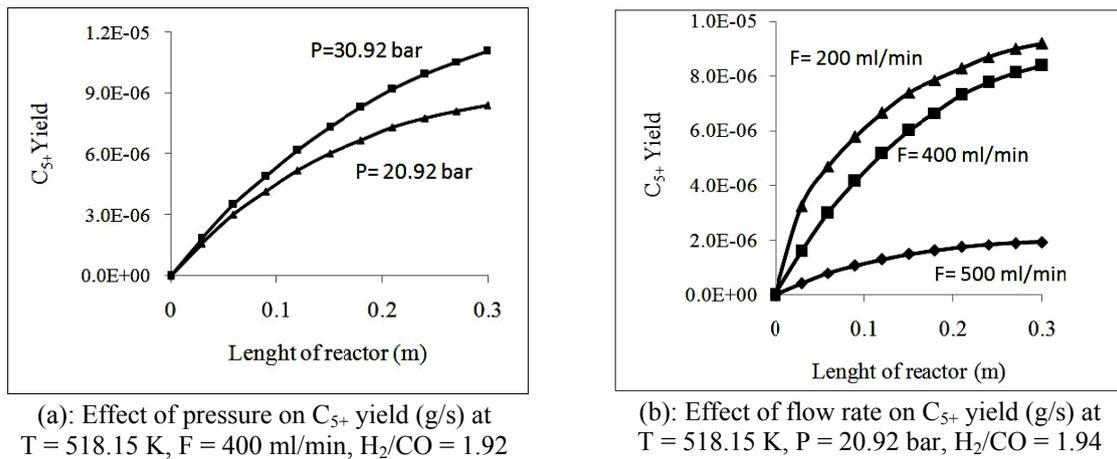
Figure 1: The effect of operating parameters on the C_{5+} yield

4. Optimization

After validating the model, the optimum conditions to maximize the flow rate of C_{5+} components in the product stream were obtained using GA. The decision variables of the optimization problem were temperature (T), pressure (P), H_2/CO ratio and CO inlet flow rate to the reactor (F_{CO}) which could vary within ranges of 493-542 K, 10.9-30.9 bar, 0.98-2.99, and 0.0815-0.3074 gmole/s, respectively. The optimization problem can be formulated as follows:

Find: T, P, H_2/CO, F_{CO}
Maximize: C_{5+} mass flow rate (g/s)
Subject to:
$493 < T < 542$ K
$10.9 < P < 30.9$ bar
$0.98 < H_2/CO < 2.99$
$0.0815 < F_{CO} < 0.3074$ gmole/s

GA is a population-based optimization algorithm based on the Darwinian survival-of-the-fittest theory. The algorithm was proposed by Holland [18] and further developed by Goldberg [19] and others. GA has been widely and successfully applied to various problems like operation research, image processing and control problems [20]. In GA, the solution procedure starts with an initial set of random solutions called population. The populations evolve through successive iterations, called generation. Each population contains a set of individuals called chromosome. Each chromosome contains a string of binary or decimal variables called gene. At each iteration, the GA randomly selects individuals from the current population as parents to produce the children for the next generation. Over successive generations, the population evolves toward an optimal solution. To create the next generation, the GA uses three operators: selection, crossover, and mutation. Selection operator selects the individuals to be parents. Crossover operator combines two parents to create children, called off-springs, for the next generation. Mutation operator applies random changes to individuals.

The main characteristic of the GA is the simultaneous evaluation of many solutions. This feature provides a wide search and it is potentially avoiding convergence to a local optimum. Some of the advantages of GA are [21]:
• Optimizes with continuous or discrete variables,
• Doesn't require derivative information,
• Simultaneously searches a wide range of feasible region of decision variables,
• Optimizes variables with extremely complex objective function,
• May encode the variables so that the optimization is done with the encoded variables, and
Works with explicit objective functions and those that their explicit form is not available

(a)   (b)

(c)   (d)

(e)   (f)
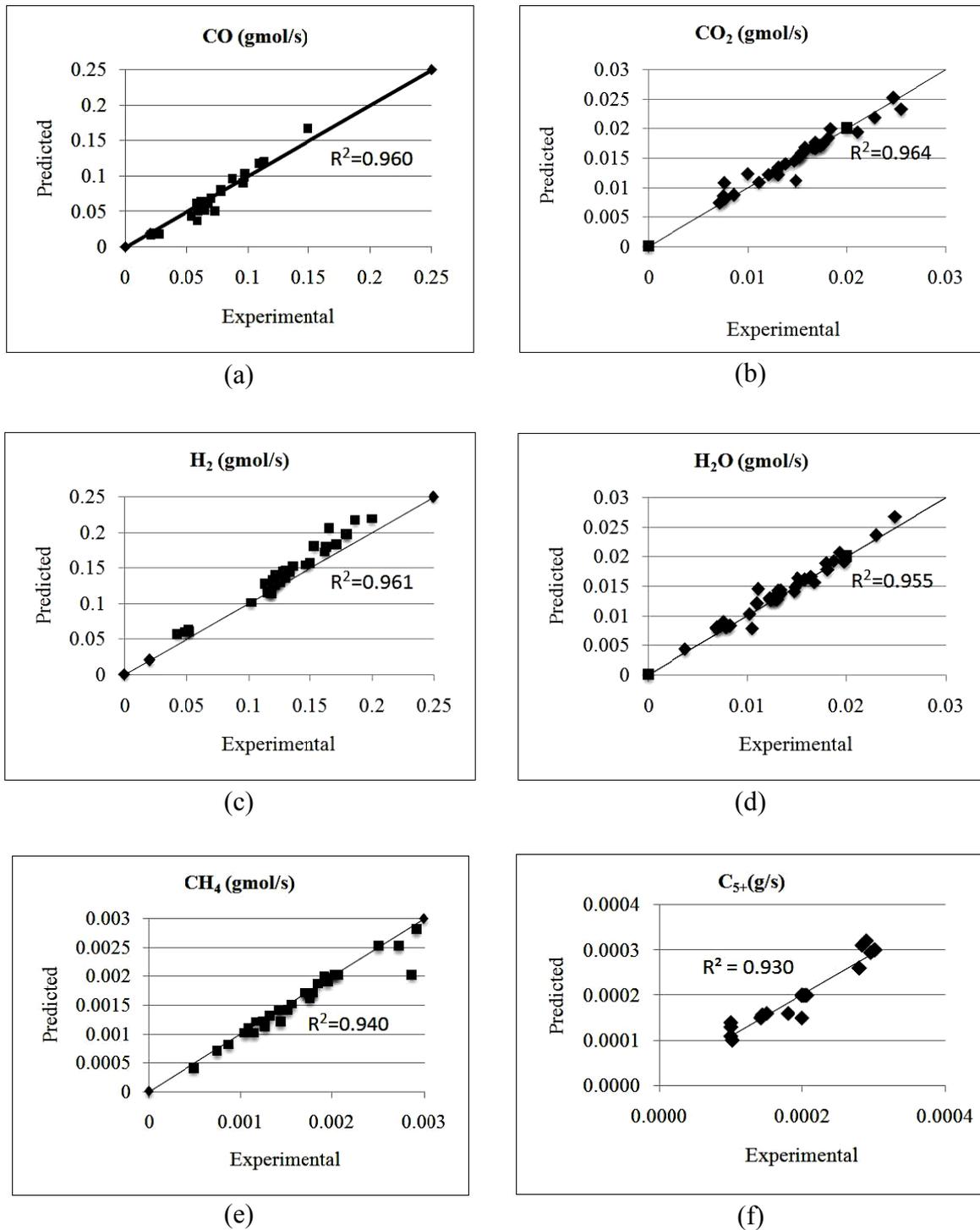
Figure 2: Comparison of model predicted product flow rates with experimental values [12] for a) CO, b) CO_2, c) H_2, d) H_2O, e) CH_4, f) C_{5+}
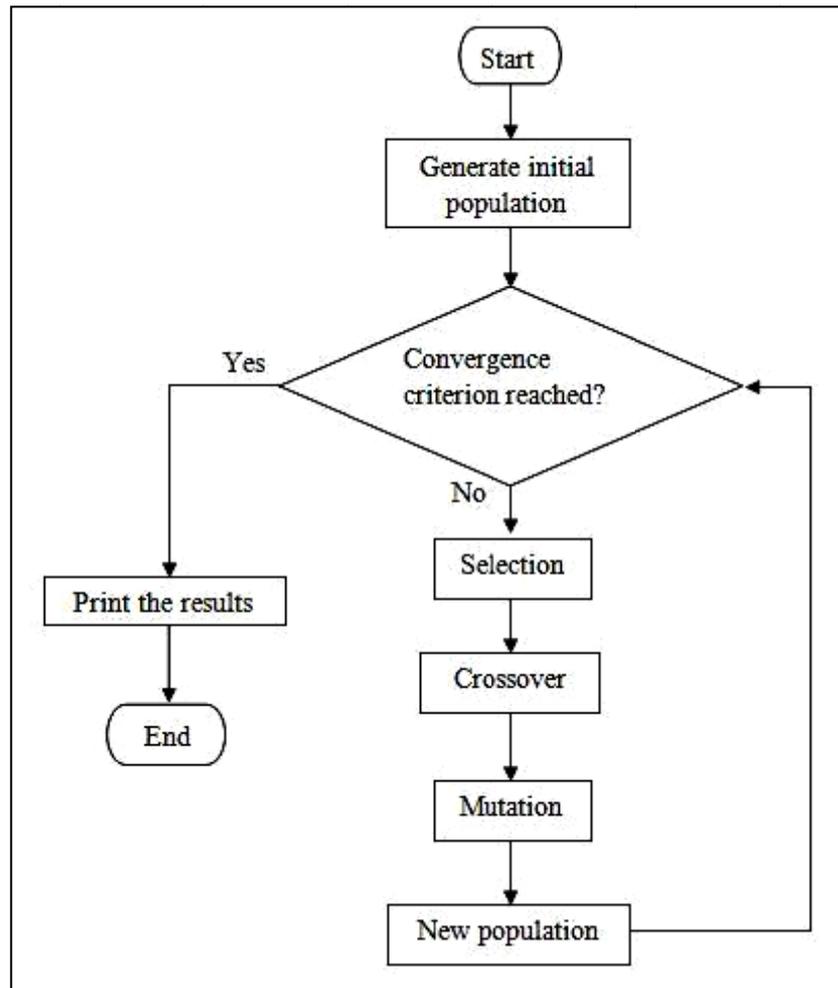
Figure 3: The general flowchart of the GA

Table 3: The best values for GA parameters

Parameter	Value
Population Size	50
Crossover Rate	70 %
Mutation Rate	10 %
No. of Generations	39

Table 4: Optimum operating conditions

Variable	Unit	Lower Bound	Upper Bound	Optimum
Pressure	Bar	10.9	30.9	30.9
Temperature	K	493	542	493
CO Molar Flow Rate in Feed Stream	gmole / s	0.0815	0.3074	0.0815
H_2/CO Ratio		0.98	2.99	0.98

In binary GA each chromosome is a binary string and only can take a value of 0 or 1. Each decision variable of the optimization problem should be mapped to a binary string whose length depends on the feasible range and the precision of the decision variable. In the problems with continuous decision variables, each variable requires many bits to be represented in binary codes. If the number of variables is large, the size of the chromosome is also large. Hence, when the variables are continuous, it is more logical to represent them by real numbers. The continuous GA also has the advantage of requiring less memory and is inherently faster than the binary GA since the chromosomes do not have to be decoded prior to the evaluation of the cost function [21]. In this paper, the continuous GA was written in MATLAB platform as all variables were continuous.

The general flowchart of the GA is presented in Figure 3. In order to select the parents, the rank weighing random pairing method was used [21]. The selection of the chromosomes would begin by ranking the individuals according to their fitness function. Then the probability of the ith chromosome in the population was calculated as follows where N_{pop} is the population size:

$$P_i = \frac{N_{pop} - i + 1}{\sum_{i=1}^{N_{pop}} i} \qquad (19)$$

After calculating the cumulative probabilities of the chromosomes, a random number between zero and one was generated. Starting at the top of the list, the first chromosome with a cumulative probability that was greater than the random number was selected as a parent. To create the off-springs from parents, arithmetic crossover was applied in which the off-springs were obtained through the following equations [21]:

$$Offspring_1 = \beta * Parent_1 + (1 - \beta) * Parent_2 \qquad (20)$$

$$Offspring_2 = \beta * Parent_2 + (1 - \beta) * Parent_1 \qquad (21)$$

where β is a random variable between zero and one.

The crossover operation was applied with a rate called crossover rate which was the percentage of off-springs that were created by crossover that usually takes a value between 60 to 80%. The rest of the off-springs of the next generation were the best chromosomes of the previous generation which transfer to the next generation without any change. The latest is called elitism which is commonly applied in GA [21]. After crossover, the mutation operator applies random changes to individuals. The mutation operator is used to ensure the diversity of the population and to avoid the GA to converge too quickly to a local minimum especially for functions which have many local minima. In this operation, some of the genes are randomly selected and then their values are replaced by new random values. The number of genes which undergo mutation is determined by the mutation rate which is the percentage of all genes that are mutated. To achieve the best solution of objective function, the GA parameters - including population size, crossover rate and mutation rate, were tuned by testing different values. These tuned values are shown in Table 3.

The production of C_{5+} was optimized using GA. The mass flow rate of C_{5+} has been chosen as objective or fitness function and the variations of both average fitness function and best fitness function in two successive generations have been chosen as convergence criteria. The algorithm converged after 39 generations. The optimum operating conditions that maximize the C_{5+} product flow rate are given in Table 4. The value of objective function (C_{5+} mass flow rate) at the optimum point was 1.58×10^{-3} g/s. It can be seen that at the optimum point, pressure is at its maximum limit while temperature, H_2/CO ratio, and F_{CO} are at their minimum limits.

5. Conclusions

The Fischer-Tropsch synthesis in a packed-bed reactor over an industrial Fe-Cu-K catalyst was modeled using a non-isothermal, one-dimensional flow reactor intrinsic reaction kinetics for both the Fischer-Tropsch and water-gas shift reactions over the above catalyst were obtained from literature and tested against the reported experimental data. Genetic algorithm optimization method was used to obtain the optimum conditions that would maximize the C_{5+} product yield. The agreement between model-predicted and experimental product yields was satisfactory. The optimum point occurred at the reactor pressure set to its maximum limit and temperature, H_2/CO ratio, and CO feed rate set at their minimum levels.

Nomenclature

A	Reactor area, m^2
C_i	Bulk gas concentrations of component i, $mol.m^{-3}$
C_0	Inlet gas concentration of component i, $mol.m^{-3}$
C_p	Residual heat capacity of ith reaction, $J.(kg.K)^{-1}$
d_{in}	Inlet tube diameter, m
d_o	Outlet tube diameter, m
d_p	Pellet diameter, m
E_5	Activation energy for paraffin formation, $kJ.mol^{-1}$
E_{5m}	Activation energy for methane formation, $kJ.mol^{-1}$
E_6	Activation energy for olefin formation, $kJ.mol^{-1}$
E_v	Activation energy for WGS reaction, $kJ.mol^{-1}$
f	Volume flow rate, $m^3.s^{-1}$
f_i	Tube fouling factor, $m^2.s.°C.J^{-1}$
f_o	Shell fouling factor, $m^2.s.°C.J^{-1}$
$-\Delta H_j$	Reaction heat of jth reaction, $J.mol^{-1}$
h_i	The tube-side heat transfer coefficient, $J.(m^2.s.K)^{-1}$
h_o	The shell-side heat transfer coefficient, $J.(m^2.s.K)^{-1}$
G	Mass velocity, $kg.m^{-2}.s^{-1}$
k_1	Rate constant of CO adsorption, $mol.g^{-1}.bar^{-1}.s^{-1}$
k_5	Rate constant of paraffin formation, $mol.g^{-1}.bar^{-1}.s^{-1}$
k_5	Pre exponential factor of paraffin formation (n≥2) , $mol.g^{-1}.bar^{-1}.s^{-1}$
k_{5m}	Pre exponential factor of rate constant of methane formation, $mol.g^{-1}.bar^{-1}.s^{-1}$
k_6	Pre exponential factor of rate constant of olefin desorption reaction, $mol.g^{-1}. s^{-1}$
k_v	Rate constant of CO_2 formation, $mol.g^{-1}.bar^{-1.5}.s^{-1}$
k_v	Pre exponential factor of rate constant of CO_2 formation, $mol.g^{-1}.bar^{-1.5}.s^{-1}$
k_{-6}	Rate constant of olefin re-adsorption reaction, $mol.g^{-1}.bar^{-1}.s^{-1}$
k_6	Rate constant of olefin desorption reaction, $mol.g^{-1}.s^{-1}$
K_1	Equilibrium constant of elementary reaction step SI for FTS reactions
K_2	Equilibrium constant of elementary reaction step SII for FTS reactions
K_3	Equilibrium constant of elementary reaction step SIII for FTS reactions
K_4	Equilibrium constant of elementary reaction step SIV for FTS reactions
K_v	Group of constants in WGS reaction, $bar^{-0.5}$
K_p	Equilibrium constant of WGS reaction
k_w	Conductivity, $W.m^{-1}.K^{-1}$
N_{pop}	Population size
NR	Number of equations
P	Total pressure, bar
P_i	Partial pressure of ith component, bar

P_{in}	Inlet reaction pressure, bar	X	Conversion
R	gas constant, $J.mol^{-1}.K^{-1}$	Z	Reactor length, m
R_j	Rate of jth reaction, mol/ g.s		Greek symbols
$R_{o,j}$	Rate of jth olefin reaction, mol/ g.s	ρ_g	Bulk gas density, kg/m^3
$R_{p,j}$	Rate of jth paraffin reaction, mol/ g.s	ρ_p	Catalyst pellet density, kg/m^3
		ε_B	Bed void age, dimensionless
$R_{co2,j}$	Rate of jth WGS reaction, mol/g.s	α_1	Chain growth factor for carbon number of 1
T_g	Bulk temperature of gas phase, K	α_n	Chain growth factor for carbon number of n (n≥2)
$T_{g,0}$	Inlet temperature of gas phases, K	α_A	Chain growth probability in the Anderson-Schulz-Flory distribution
T_{cold}	Cooling temperature, K		
T_w	Wall temperature, K		
u_s	Superficial gas velocity, m/s	β_n	Re-adsorption factor of 1-olefin with carbon number of n
U	Overall heat transfer coefficient, $J/m^2.s.K$		

References:

1- Wang, Y. N., Xu, Y. Y., Li, Y. W., Zhao, Y. L. and Zhang, B. J. (2003). "Heterogeneous modeling for fixed bed reactor for Fischer-Tropsch synthesis: Reactor model and its applications." *Chemical Engineering Science*, Vol. 58, PP. 867-875.

2- Anastai, J. L. (1980). "SASOL: South Africa's oil from coal story - background for environmental assessment." U.S. EPA report 600/8-80-002.

3- Sie, S. T. and Krishna, R. (1999). "Fundamentals and selection of advanced Fischer–Tropsch reactors." *Applied Catalysis A: General,* Vol. 186, PP. 55-70.

4- Jess, A. and Kern, C. (2009). "Modeling of multi-tubular reactors for Fischer-Tropsch synthesis." *Chemical Engineering Technology,* Vol. 32, PP. 1164-1175.

5- Rafiq, M. H., Jakobsen, H. A., Schmid, R. and Hustad, J. E. (2011). "Experimental studies and modeling of a fixed bed reactor for Fischer-Tropsch synthesis using biosyngas." *Fuel Processing Technology,* Vol. 92, PP. 893-907.

6- Fernandes, F. A. N. and Teles, U. M. (2007). "Modeling and optimization of Fischer–Tropsch products hydrocracking." *Fuel Processing Technology,* Vol. 88, PP. 207-214.

7- Fernandes, F. A. N. (2005). "Polymerization kinetics of Fischer-Tropsch reaction on iron based catalyst and product grade optimization." *Chemical Engineering Technology,* Vol. 28, PP. 930-938.

8- Wang, Y., Fan, W., Liu, Y., Zeng, Z., Hao, X., Changa, M., Zhang, C., Xu, Y., Xiang, H. and Li, Y. (2008). "Modeling of the Fischer–Tropsch synthesis in slurry bubble column reactors." *Chemical Engineering and Processing*, Vol. 47, PP. 222–228.

9- Schweitzer, J. M. and Viguié, J. C. (2009). "Reactor modeling of a slurry bubble column for Fischer-Tropsch synthesis." *Oil & Gas Science and Technology*, Vol. 64, PP. 63-77.

10- Fernandes, F. A. N. (2006). "Modeling and product grade optimization of Fischer - Tropsch synthesis in a slurry reactor." *Industrial Engineering & Chemistry Research*, Vol. 45, PP. 1047-1057.

11- Sehabiague, L., Lemoine, R., Behkish, A., Heintz, Y. J., Sanoja, M., Oukaci, R. and Morsi, B. I. (2008). "Modeling and optimization of a large-scale slurry bubble column reactor for producing 10,000 bbl/day of Fischer-Tropsch liquid hydrocarbons." *Journal of the Chinese Institute of Chemical Engineers*, Vol. 39, PP. 169-179.

12- Wang, Y. N., Ma, W. P., Lu, Y. J., Yang, J., Xu, Y. Y., Xiang, H. W., Li, Y. W., Zhao, Y. L. and Zhang, B. J. (2003). "Kinetics modelling of Fischer-Tropsch synthesis over an industrial Fe-Cu-K catalyst." *Fuel*, Vol. 82, PP. 195-213.

13- Froment, G. F. and Bischoff, K. B. (1979). *Chemical reactor analysis and design*. 1st Ed. John Wiley & Sons, New Jersey, USA.

14- Steynberg, A. P. and Dry, M. E. (2004). *In Studies in Surface Science and Catalysis: Fischer-Tropsch Technology*. 1st Ed. Elsevier, Amsterdam, Netherlands.

15- Holman, J. P. (1997). *Heat transfer*. 8th Ed. McGraw Hill, USA.

16- Megyesy, E. F. (2001). *Pressure Vessel Handbook*. 12th Ed. Pressure Vessel Publishing, Tulsa, Oklahoma, USA.

17- Ludwig, E. E. (1990). *Applied process design for chemical and petrochemical plants*. Vol 3, 3rd Ed. Gulf Professional Publishing, Oxford, United Kingdom.

18- Holland, J. H. (1975). *Adaptation in natural and artificial systems*. 1st Ed. University of Michigan Press, Ann Arbor, USA.

19- Goldberg, D. E. (1989). *Genetic algorithms in search, optimization and machine learning*. 1st Ed. Addison Wesley, Boston, USA.

20- Hwang, S. and He, R. (2006). "A hybrid real-parameter genetic algorithm for function optimization." *Advanced Engineering Informatics*, Vol. 20, PP. 7-21.

21- Haupt, R. L. and Haupt, S. E. (2004). *Practical genetic algorithms*. 2nd Ed. John-Wiley & Sons, New Jersey, USA.